J.-S. Lönnroth, V. Parail, C. Figarella, X. Garbet, G. Corrigan, D. Heading, and JET-EFDA Contributors. 2004. Predictive modelling of ELMy H-modes with a new theory-motivated model for ELMs. Plasma Physics and Controlled Fusion, volume 46, number 5A, pages A249-A256.

http://www.iop.org/journals/ppcf
http://stacks.iop.org/ppcf/46/A249

INSTITUTE OF PHYSICS PUBLISHING PLASMA PHYSICS AND CONTROLLED FUSION

Plasma Phys. Control. Fusion **46** (2004) A249–A256 PII: S0741-3335(04)70003-2

Predictive modelling of ELMy H-modes with a new theory-motivated model for ELMs

J-S Lönnroth[1], V Parail[2], C Figarella[3], X Garbet[3], G Corrigan[2], D Heading[2] and JET-EFDA Contributors

[1] Association EURATOM-Tekes, Helsinki University of Technology, PO Box 2200, 02015 HUT, Finland
[2] EURATOM/UKAEA Fusion Association, Culham Science Centre, Abingdon, Oxfordshire OX14 3DB, UK
[3] Association EURATOM-CEA, CEA Cadarache, DRFC, 13108 Saint-Paul-Lez-Durance, France

Received 8 October 2003
Published 21 April 2004
Online at stacks.iop.org/PPCF/46/A249
DOI: 10.1088/0741-3335/46/5A/027

Abstract

A new model for the type I ELMy H-mode based on linear ballooning stability theory is presented. The model can be written as a linear differential equation for the amplitude of an unstable ballooning mode and is coupled to a system of transport equations. The differential equation for the ballooning mode amplitude has two terms—one representing the growth rate of the perturbation and one controlling the decay rate of the mode and driving the mode amplitude towards the level of background fluctuations. A critical pressure gradient limit is used to control whether the growth rate differs from zero. When coupled to a JETTO transport simulation, the model qualitatively reproduces the experimental dynamics of a type I ELMy H-mode, including an edge localized mode (ELM) frequency that increases with the external heating power. This paper also discusses why the linear ballooning model, in the first place, produces discrete oscillations when coupled to a transport simulation rather than a stationary state with a slightly enhanced ballooning mode amplitude.

1. Introduction

A plasma in a tokamak operating in the high confinement mode (H-mode) is generally characterized by the formation of an edge transport barrier (ETB), a narrow edge region with reduced transport typically featuring strong periodic discharges of particles and energy called edge localized modes (ELMs). ELMs are broadly believed to be controlled by ballooning and peeling/kink mode magnetohydrodynamic (MHD) instabilities [1–5], the former being driven mainly by the edge pressure gradient and the latter mainly by the edge current. The most common type of ELMs, called type I ELMs, have been observed for a wide range of densities in plasmas with modest and strong external heating. Type I ELMs, which are the most violent type of ELM disruptions, can remove up to 10% of the plasma energy in a single ELM. They

are characterized by an ELM frequency that increases with the radial power flux across the last closed flux surface and a high level of confinement. The type I ELMy H-mode is generally regarded as a reference scenario for the International Thermonuclear Experimental Reactor (ITER) and other future burning plasma experiments.

2. Analytical linear ballooning model for type I ELMs

This paper presents a model for the type I ELMy H-mode based on linear ballooning mode theory. It is assumed that the ballooning modes are controlled mainly by the edge pressure gradient. The construction of the new model has been inspired by and is analogous to the construction of the model

$$\frac{\mathrm{d}\xi}{\mathrm{d}t} = \lambda(|p'| - |p'_c| + av_\theta^2 - bv_E'^2)\xi \tag{1}$$

used by Lebedev *et al* in [6]. Here, ξ is the mean square level of MHD velocity fluctuations, t is the time and the expression in front of ξ on the right-hand side corresponds to the growth rate of the ballooning instability. The quantity λ is a constant characterizing the growth rate, p' is the pressure gradient and p'_c is a critical pressure gradient threshold, above which the instability starts to grow. The last two terms inside the parenthesis represent corrections due to poloidal rotation and the shear in the flow of poloidal velocity of $\boldsymbol{E} \times \boldsymbol{B}$ motion, respectively, both of which modify the stability threshold.

Similarly, the model used in this paper is a minimal model for describing the linear evolution of the ballooning mode amplitude. The ELMs are represented by exponentially growing fluctuations in a simple linear MHD model for a system with a background thermal noise. The following linear differential equation has been constructed for the ballooning mode amplitude:

$$\frac{\mathrm{d}\xi}{\mathrm{d}t} = C_1 \frac{c_s}{\sqrt{L_p R}} \left(1 - \frac{\alpha_c}{\alpha}\right) H\left(1 - \frac{\alpha_c}{\alpha}\right) \xi - C_2 \frac{c_s}{R}(\xi - \xi_0). \tag{2}$$

Here, $C_1 \sim 1$, $C_2 \sim 0.1$ and $\xi_0 \sim 0.01$ are constants characterizing the growth rate of the instability, the decay rate of the mode due to non-ideal MHD effects and the level of background fluctuations, respectively, H is the Heaviside function defined as $H(x) = 0$, if $x < 0$ and $H(x) = 1$, if $x \geqslant 0$, x being an arbitrary variable, $c_s = \sqrt{T_e/m_i}$ is the speed of sound, where T_e is the electron temperature and m_i is the ion mass, $L_p = p/|\mathrm{d}p/\mathrm{d}r|$ is the pressure scale length, where p is the pressure, r the minor radius and R is the major radius; $\alpha = -(2\mu_0 r^2/B_\theta)(\mathrm{d}p/\mathrm{d}\psi)/0.64$ is the normalized pressure gradient, where B_θ is the poloidal magnetic field, ψ the poloidal flux coordinate and α_c is the critical normalized pressure gradient.

In equation (2), the corrections to the critical pressure gradient threshold used in equation (1) have been omitted for simplicity. Above the threshold α_c, the mode amplitude increases linearly with a growth rate equal to the ballooning mode growth rate. The factor $c_s/\sqrt{L_p R}$ corresponds to the ballooning mode growth rate well above the instability threshold. Below the threshold α_c, the growth rate is zero due to the Heaviside function, which has been introduced in the model to account for the fact that there is no damping or growing solution in ideal MHD with $\alpha < \alpha_c$. Introducing the Heaviside function is a simple way of reproducing the transition from an oscillating solution to a growing solution taking place when the critical pressure gradient is exceeded. The second term on the right-hand side of equation (2) has been introduced to describe the level of background fluctuations and the decay rate of the mode after an ELM crash due to non-ideal MHD effects. This additional term causes the mode amplitude to tend to converge towards the level of background fluctuations between the ELMs.

The coefficient $C_2 c_s/R$ determines the rate at which the mode is damped after an ELM crash by, e.g., finite viscosity, diffusivity and other non-ideal MHD effects. The coefficients C_1, C_2 and ξ_0 have been chosen so that a regime of ELM generation is obtained. The choice of the coefficients C_1 and C_2 so that $C_1 \sim 1$ and $C_2 \ll C_1$ goes in line with what would be expected from a general description of the ballooning instability.

3. JETTO implementation

The analytical linear ballooning model defined by equation (2) has been implemented in the 1.5D JETTO transport code [7]. JETTO uses the semi-empirical JET transport model, which is a mixed Bohm/gyro-Bohm model [8]. The ETB is represented by a sudden reduction of the transport coefficients to a uniform neo-classical level in a 3 cm wide region at the edge of the plasma. With this choice of parameters, the top of the ETB is located at about $\rho = 0.935$, where ρ is the toroidal flux co-ordinate. The width of the ETB does not play an essential role in determining whether the model yields discrete ELMs or not when coupled to a transport simulation and is, therefore, considered an external fixed parameter. The effect of letting the ETB width vary has been studied in [9].

At each time step, the (normalized) pressure gradient, pressure scale length and temperature calculated by JETTO are used to evaluate the perturbation amplitude ξ, and Gaussian-shaped perturbations having amplitudes proportional to the perturbation amplitude ξ given by equation (2) are added on top of the radial profiles of the transport coefficients within the ETB and in its vicinity. Specifically, the additional transport perturbation $\delta\chi$ representing ELMs can be written

$$\delta\chi(r,t) \sim \xi(t) \exp\left[-\left(\frac{r-r_0}{\Delta}\right)^2\right], \tag{3}$$

where r_0 is the radial location of the centre of the Gaussian and Δ is the characteristic width of the Gaussian. In this way, JETTO and the ELM model are coupled to each other through a feedback loop working in both directions. The use of Gaussian-shaped ELMs is motivated by the fact that the ballooning modes assumed to drive the ELMs have Gaussian shapes in linear theory.

The fact that the perturbations applied to the transport coefficients scale linearly with the calculated ballooning mode amplitude is consistent with the commonly used quasi-linear approximation [10]. In the mixing length approximation [10], which corresponds to a strong turbulence limit, the thermal conductivities and particle diffusivity scale as $\chi \sim \lambda_w^2 \gamma_d \sim \gamma_d / k_\perp^2$. Here, λ_w is the characteristic wavelength of the turbulence, γ_d is the decorrelation rate, which scales in the same way as the growth rate of the instability, and $k_\perp$ is the perpendicular wavenumber. Therefore, the enhancement of the transport coefficients should arguably scale with the ballooning mode amplitude as something in the range from almost no dependence, consistent with the constant saturated level of diffusivity in the strong turbulence limit, to the square dependence given by the quasi-linear approximation. The linear dependence used in this paper lies in between these two extremes and gives qualitatively the same results as the quadratic dependence.

In JETTO, the terms on the right-hand side of the differential equation are treated as averages over the whole ETB:

$$\frac{\mathrm{d}\xi}{\mathrm{d}t} = \frac{1}{N} \sum_{i=i_{\text{top of ETB}}}^{i_{\text{edge}}} \left[C_1 \frac{c_{si}}{\sqrt{L_{pi} R_i}} \left(1 - \frac{\alpha_c}{\alpha_i}\right) H\left(1 - \frac{\alpha_c}{\alpha_i}\right) \xi - C_2 \frac{c_{si}}{R_i} (\xi - \xi_0) \right]. \tag{4}$$

Here, the sums runs over all mesh points within the ETB, the index i refers to the mesh point number and N is the number of mesh points within the ETB in the JETTO grid. Averaging equation (2) over the ETB is justified, because there is toroidal coupling in place between the individual harmonics making up a ballooning mode, so that the mode can be considered global. The choice that the radial extent of the unstable mode usually coincides with the ETB width has been cross-checked in numerical analysis with the MHD stability code MISHKA [11].

For simplicity, the critical normalized pressure gradient α_c is radially constant in the simulations discussed in this paper. Some description of how the most important types of ELMy H-modes are controlled by various MHD stability limits is given in [12]. Using the MHD stability codes HELENA and MISHKA [13], it is shown in [12] that type I ELMy H-mode discharges, in general, enter the second ballooning stability region, whereby stability is solely determined by the finite-n ballooning stability limit. The analysis self-consistently takes into account how ballooning stability is influenced by a sequence of causalities involving the edge density, collisionality, bootstrap current and magnetic shear. The fixed value $\alpha_c = 1.5$ used in this paper has been chosen so that it corresponds fairly well to the finite-n ballooning stability limit relevant for a type I ELMy H-mode. In some circumstances, the location of the finite-n ballooning stability limit in terms of α varies relatively little across the ETB, as assumed here, but it is often the case that the limit moves towards larger α with increasing proximity to the separatrix. This should, strictly speaking, translate into a critical pressure gradient that increases towards the separatrix. Introducing such a non-uniform critical pressure gradient in the model quantitatively leads to a lower ELM frequency, which can be understood in light of the ELM generation mechanism presented in the following section. Determining exactly how α_c should vary across the ETB is, however, beyond the scope of this paper, which aims to demonstrate the functionality of the ELM model given by equation (2) and to explain the ELM generation mechanism of the model.

4. Obtaining oscillations with a linear ballooning model

It is generally not easy to find self-oscillating solutions to systems consisting of a simple model of instability, such as equation (2), coupled to a set of transport equations. Several conditions have to be satisfied in order to obtain discrete oscillations with a model like equation (2). To begin with, it seems as if no oscillations can be obtained in a zero-dimensional system and it is essential that the model is coupled to a transport simulation, as in this paper. It also seems to be necessary that the ELMs are represented by perturbations with a finite width, e.g. by using Gaussian-shaped eigenfunctions as here. In addition, it seems to be of some importance that the model is treated as an average over the whole ETB, as in equation (4), but oscillations have in some cases been obtained even when evaluating equation (2) at just a single mesh point. The fact that the model uses a Heaviside function in the growth rate term might also be important. The Heaviside function prevents the growth rate from becoming negative, which corresponds to an ideal MHD nature of the instability.

Apart from these factors, the onset of discrete oscillations is related to how the radial profiles of the transport coefficients are perturbed in the transport simulation under inspection and to how the pressure gradient evolves as a result of this. In order to demonstrate the effect, three different predictive JETTO simulations with qualitatively different ELM behaviour will be considered. In each of the three cases, the ELM perturbation is the part of a 6 cm wide Gaussian that fits inside the simulation region given the specific location and width of the eigenfunction. The critical normalized pressure gradient is $\alpha_c = 1.5$. Figure 1 shows the ion thermal conductivity at the magnetic surface with the largest ELM amplitude as a function of time in the three simulations. The simulation parameters differ only with respect to the

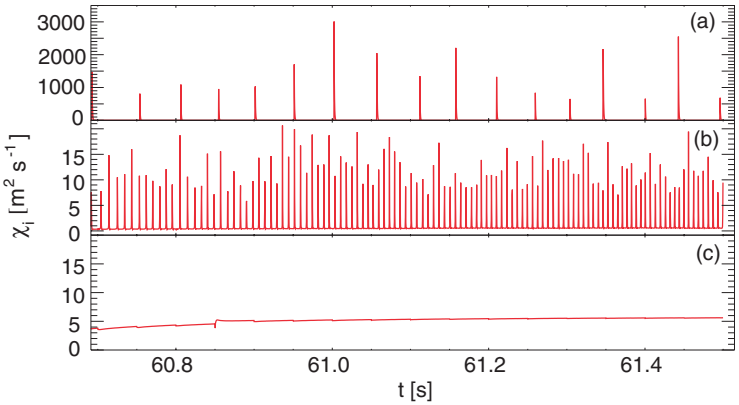

Figure 1. Time traces of the ion thermal conductivity in three predictive JETTO simulations with Gaussian-shaped ELM perturbations having the same characteristic width of 6 cm in each case, but centred at different radial locations in the three runs. Specifically, the ELM perturbations are centred at the following radial locations: (*a*) $\rho = 0.92$, (*b*) $\rho = 0.95$, (*c*) $\rho = 0.98$. The time traces correspond to the flux surface at which the ELM perturbation is centred.

positioning of the ELM perturbation, which is centred at $\rho = 0.92$ in frame (*a*), at $\rho = 0.95$ in frame (*b*) and at $\rho = 0.98$ in frame (*c*). Primarily as a result of the positioning of the perturbation, the case in frame (*a*) has discrete very strong ELMs, the case in frame (*b*) discrete small and frequent ELMs and the case in frame (*c*) a small continuous enhancement of transport.

Figure 2 helps to explain the results shown in figure 1. Frame (*a*) shows how the ion thermal conductivity χ_i evolves as a function of time at six equidistant radial locations ($\rho = 0.94$, $\rho = 0.95$, $\rho = 0.96$, $\rho = 0.97$, $\rho = 0.98$ and $\rho = 0.99$) within the ETB before, during and after one of the strong ELMs obtained with the perturbation centred at $\rho = 0.92$. The profiles of electron thermal conductivity and particle diffusivity are perturbed in the same way and thus have a similar time evolution. Because the perturbation is centred quite far inside the plasma, the level of transport decreases strongly towards the edge of the pedestal, where it approaches the neo-classical level. Due to the very high level of transport near the top of the pedestal, heat and particles quickly diffuse towards the edge. Because the level of transport decreases towards the edge, the diffusion gets weaker there and as a result the pressure gradient starts to increase due to the accumulation of heat and particles. This is illustrated in frame (*b*), which shows time traces of the normalized pressure gradient α for the same equidistant radii as χ_i in frame (*a*). As seen in the figure, the peak in the normalized pressure gradient continually increases as it propagates towards the edge during the ELM, because transport decreases radially all the time. It is the propagation and strong build-up of the peak in the normalized pressure gradient that keeps feeding the growth of the instability, so that the critical normalized pressure gradient is exceeded somewhere within the ETB long enough and the growth rate of the exponentially growing perturbation becomes large enough for a very strong ELM to develop. It should be noted that the normalized pressure gradient reaches a maximum level of $\alpha = 2.35$ at $\rho = 0.99$, which is way above the critical level $\alpha_c = 1.5$. Closer to the separatrix, the maximum value becomes even higher. It takes a very strong ELM to eventually deplete this peak. Another interesting feature partly visible in frame (*b*) is that the normalized pressure gradient exceeds the critical level $\alpha_c = 1.5$ long before the onset of the sharp distinct peak in the level of transport, which occurs only when the peak in the pressure gradient starts to build-up at the edge. The complete ELM is thus a lengthy phenomenon.

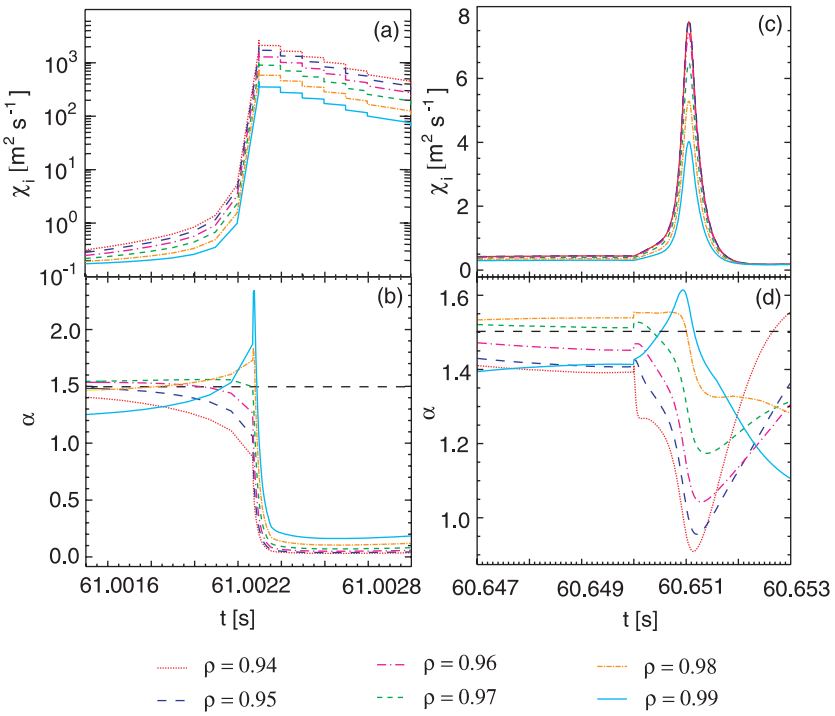

Figure 2. (*a*) Time traces of the ion thermal conductivity at flux surfaces $\rho = 0.94$, $\rho = 0.95$, $\rho = 0.96$, $\rho = 0.97$, $\rho = 0.98$ and $\rho = 0.99$ within the ETB before, during and after one of the strong ELMs in frame (*a*) in figure 1. (*b*) Time traces of the normalized pressure gradient at the same flux surfaces and for the same time interval. The critical level of the normalized pressure gradient has been marked with a dashed line. (*c*) Time traces of the ion thermal conductivity at the same flux surfaces as in frame (*a*) before, during and after one of the small ELMs in frame (*b*) in figure 1. (*d*) Time traces of the normalized pressure gradient at the same flux surfaces and for the same time interval.

Frames (*c*) and (*d*) in figure 2 show a similar analysis for one of the small ELMs in the simulation with the ELM centred at $\rho = 0.95$. As shown in frame (*c*) for the ion thermal conductivity, the transport coefficients vary much more modestly across the pedestal than in frame (*a*), because the perturbation is centred closer to the edge and its amplitude stays smaller. In particular, when centred at $\rho = 0.95$ the perturbation plays a more important role at the separatrix than when centred at $\rho = 0.92$. Since the ratio of the maximum level of transport in the pedestal to the level of transport just inside the separatrix is reasonably small, the effect of generating a propagating and growing peak in the pressure gradient at the edge is modest, as shown in frame (*d*) with time traces of the normalized pressure gradient. The mechanism feeding the growth of the instability is thus significantly suppressed, but still exists, enabling a discrete oscillation to take place. As a result of the smaller achieved level of the normalized pressure gradient, the growth rate stays moderate and the perturbation stops growing fairly quickly. The small ELM causes a relatively modest collapse of the pressure gradient, from which the system quickly recovers and enters the lengthy build-up phase culminating in the next discrete oscillation. The normalized pressure gradient drops below the critical level only momentarily after each small ELM.

It is now easy to understand why centring the ELM perturbation at $\rho = 0.98$ results in a continuous ELM, as shown in frame (*c*) in figure 1. With this choice of ELM positioning, a

discrete ELM would enhance transport very significantly at the edge and transport would vary relatively little across the pedestal. Hence, the growing and propagating peak in the pressure gradient at the edge, which seems to be necessary in order to obtain a discrete ELM, cannot develop. Instead, the system settles into a steady state with the normalized pressure gradient marginally exceeding the critical level just outside the top of the ETB and a resulting small continuous enhancement of transport.

5. Reproducing the dynamics of the type I ELMy H-mode

The linear ballooning model for ELMs presented in this paper is capable of qualitatively reproducing the main features of the type I ELMy H-mode when coupled to a JETTO transport simulation. With an appropriate choice of simulation parameters, such a simulation produces strong periodic oscillations with a repetition frequency that increases with the external heating power. This is illustrated in figure 3, which shows time traces of the ion thermal conductivity at the magnetic surface $\rho = 0.94$ slightly outside the top of the ETB at $\rho = 0.93$ in five predictive transport simulations with different levels of neutral beam heating power. The plots distinctly resemble time traces of the D_α signal in type I ELMy H-mode discharges. In these particular simulations, the transport perturbation representing an ELM is a Gaussian that has a characteristic width of a 6 cm and is centred at the magnetic surface $\rho = 0.94$. In the cases of ion and electron thermal conductivities as well as in the case of particle diffusivity, the amplitude of the Gaussian-shaped ELM perturbation is the neo-classical level times ξ given by equation (4). The edge density in the simulation is $n_0 = 1 \times 10^{19}\,\mathrm{m}^{-3}$ and the edge temperature $T_0 = 100\,\mathrm{eV}$ for both electrons and ions, the values being typical for the type I

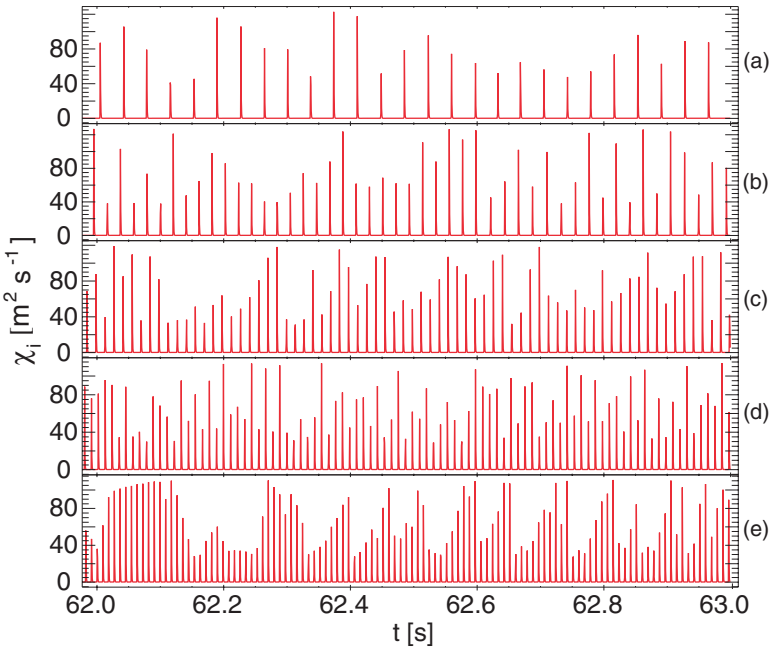

Figure 3. Time traces of the ion thermal conductivity at the magnetic surface $\rho = 0.94$ in five predictive JETTO simulations with different levels of external heating power: (*a*) $P = 4\,\mathrm{MW}$, (*b*) $P = 8\,\mathrm{MW}$, (*c*) $P = 12\,\mathrm{MW}$, (*d*) $P = 16\,\mathrm{MW}$, (*e*) $P = 20\,\mathrm{MW}$.

ELMy H-mode. The simulations have been run for 0.5 s in the L-mode before the transition to the H-mode. The neutral beam heating power varies from $P = 4\,\mathrm{MW}$ to $P = 20\,\mathrm{MW}$ in steps of 4 MW in the simulations shown in frames (*a*)–(*e*) in figure 3. As in experiments with the type I ELMy H-mode, the ELM frequency slowly increases with the heating power. The feature that the ELM frequency increases with increasing external heating power can be attributed to the fact that the recovery time between the ELMs decreases with increasing power and can, therefore, be reproduced in simulations with many simple ELM models.

6. Summary and discussion

This paper has presented an analytical model for the type I ELMy H-mode based on the linear ballooning stability theory. The model can be written as a simple linear differential equation for the perturbation amplitude. One term in the differential equation represents the growth rate of the perturbation and another one controls the decay rate of the mode due to non-ideal MHD effects and drives the mode amplitude towards the level of background fluctuations. The growth rate term in the equation remains zero as long as the pressure gradient does not exceed a critical value used to define the model. By coupling the linear ballooning model into a transport simulation and treating the differential equation as an average over the whole ETB, the experimental dynamics of the type I ELMy H-mode can be qualitatively reproduced. In particular, simulations with the model reproduce a type I ELM frequency that increases with the external heating power, as in experiments. It has been demonstrated that in the first place the onset of discrete oscillations is related to how the radial profiles of the transport coefficients are perturbed in the transport simulation and to how the pressure gradient evolves as a result of this. Finally, it should be remembered that in a real plasma the evolution of the current may destabilize peeling modes, which may also play a role in triggering the ELMs. To extend the ballooning model proposed in this work to take into account mainly current-driven peeling instabilities is left for future work.

Acknowledgment

This work has been performed under the European Fusion Development Agreement.

References

[1] Huysmans G T A, Hender T and Alper B 1998 *Nucl. Fusion* **38** 179
[2] Connor J W, Hastie R J, Wilson H R and Miller R L 1998 *Phys. Plasmas* **5** 2687
[3] Rogers B N and Drake J F 1999 *Phys. Plasmas* **6** 2797
[4] Hastie R J, Catto P J and Ramos J J 2000 *Phys. Plasmas* **7** 4561
[5] Snyder P B *et al* 2002 *Phys. Plasmas* **9** 2037
[6] Lebedev V B *et al* 1995 *Phys. Plasmas* **2** 3345
[7] Cennachi G and Taroni A 1988 JET-IR(88)03
[8] Erba M *et al* 1997 *Plasma Phys. Control. Fusion* **39** 261
[9] Onjun T, Bateman G, Kritz A H and Hammet G 2002 *Phys. Plasmas* **9** 5018
[10] Weiland J 2000 *Collective Modes in Inhomogeneous Plasmas* (Bristol: Institute of Physics Publishing)
[11] Huysmans G T A, Sharapov S E, Mikhailovskii A B and Kerner W 2001 *Phys. Plasmas* **10** 4292
[12] Lönnroth J-S *et al* 2003 *Plasma Phys. Control. Fusion* **45** 1689
[13] Mikhailovskii A B *et al* 1997 *Plasma Phys. Rep.* **23** 844